

Scanning flow cytometer modified to distinguish phytoplankton cells from their effective size, effective refractive index, depolarization, and fluorescence

Luca Fiorani,^{1,*} Valeri P. Maltsev,^{2,3,4} Vyacheslav M. Nekrasov,^{2,3} Antonio Palucci,¹ Konstantin A. Semyanov,² and Valeria Spizzichino¹

¹Laser Applications Section, Italian Agency for New Technologies, Energy and the Environment (ENEA), Fermi Street 45, 00044 Frascati, Italy

²Institute of Chemical Kinetics and Combustion, SB RAS, Institutskaya Street 3, 630090 Novosibirsk, Russia

³Novosibirsk State University, Pirogova Street 2, 630090 Novosibirsk, Russia

⁴State Research Center of Virology and Biotechnology VECTOR, 630559 Koltsovo, Russia

*Corresponding author: fiorani@frascati.enea.it

Received 7 May 2008; accepted 13 July 2008;
posted 17 July 2008 (Doc. ID 95848); published 19 August 2008

A laser flow cytometer based on scanning flow cytometry has been assembled. The unpolarized and linearly polarized light-scattering profiles, as well as the side emitted light in different spectral bands, were measured, allowing the simultaneous and real-time determination of the effective size and the effective refractive index of each spherelike particle. Additionally, each particle could be identified from depolarization and fluorescence measured simultaneously. The tests with aqueous samples of polystyrene spheres, fluorescent or nonfluorescent, and phytoplankton cells demonstrate that the system is able to retrieve size and refractive index with an accuracy of 1% and that the depolarization and fluorescence measurements allow the classification of particles otherwise indistinguishable. © 2008 Optical Society of America

OCIS codes: 120.5820, 170.1530, 300.2530.

1. Introduction

The simultaneous measurement of effective size and effective refractive index of microscopic spherical particles by laser systems is based on the Mie theory that describes light scattering by dielectric spheres [1]. In general the instruments based on this technique are named laser particle counters [2] and laser flow cytometers [3], if the particles are suspended in air and water, respectively. The great interest for the fast classification of microscopic particles in liquid suspensions (e.g., marine phytoplankton and

blood cells) favored the broad diffusion of commercial systems based on laser flow cytometry (LFC).

In usual LFC the particle flow and the laser beam are orthogonal. When a particle crosses the beam, the radiation is scattered with an angular distribution that depends on size and refractive index. In general, in commercial systems only forward-scattering cytometry (FSC) and side-scattering cytometry (SSC) are measured, without retrieving the size and the refractive index. Often, the particle fluorescence is detected in some spectral bands. Forward scattering is associated with the particle size [4]; side scattering is dominated by refractive effects [5]. Although they are simplifications, this approach allows the fast classification of cells both in

oceanographic [6] and clinical [7] fields, especially if the cells are marked with monoclonal antibodies conjugated to fluorescent dyes.

Typically LFC allows one to simultaneously acquire five parameters: forward scattering, side scattering, and fluorescence in three spectral bands. The counting rate can exceed 10,000 particles/s.

Recently this has been realized through CLASS, a laser flow cytometer for the characterization of phytoplankton cells, at the laboratories of Frascati of the Laser Application Section (LAS) of the Italian Agency for New Technologies, Energy and the Environment, in collaboration with the Institute of Chemical Kinetics and Combustion (ICKC) in Novosibirsk, Russia.

Taking into account that

- phytoplankton cells can be discriminated not only by size and refractive index, but also via shape and pigmentation, and
- shape and pigmentation can be observed thanks to scattering depolarization and fluorescent emission, respectively,

it has followed a research line, allowing one to reach the objective consisting of the simultaneous determination of the effective size and the refractive index of spherelike particles from the solution of the inverse light-scattering problem and measurement of the depolarization and fluorescence of microscopic particles.

In this respect, LAS and ICKC have carried out complementary research for more than a decade: LAS developed local and remote sensors based on laser-induced fluorescence (LIF) for bio-optical measurements of natural waters [8,9], and ICKC demonstrated applicability of the scanning flow cytometry (SFC) in analysis of different particles [10–12]. Both research lines resulted in prototype patents [13,14]. Eventually combining LIF, SFC, and polarizing optics was developed through CLASS, an innovative system able to simultaneously measure fluorescence and two angular dependencies of light-scattering intensities of microscopic particles in liquid suspension. We will illustrate the operation of CLASS describing the measurement of a sample of *Chlamydomonas reinhardtii*, a eukaryote single-cell green alga.

2. Instruments and Methods

CLASS represents the first application of SFC to phytoplankton cells [15]. The optical scheme of CLASS is shown in Fig. 1; the optical elements are described in Table 1. To measure two angular dependencies of light-scattering intensities, it has been necessary to use a diode laser with a high polarization ratio (100:1). Moreover, such a source is characterized by large power and short wavelength, allowing the system to have good sensitivity and to detect sub-micrometric particles (up to about half of the wavelength). Potentially it is possible to increase the polarization ratio inserting in the beam a Thorlabs GT10 Glan Taylor polarizer (clear aperture diameter of 10 mm and extinction ratio of 100,000:

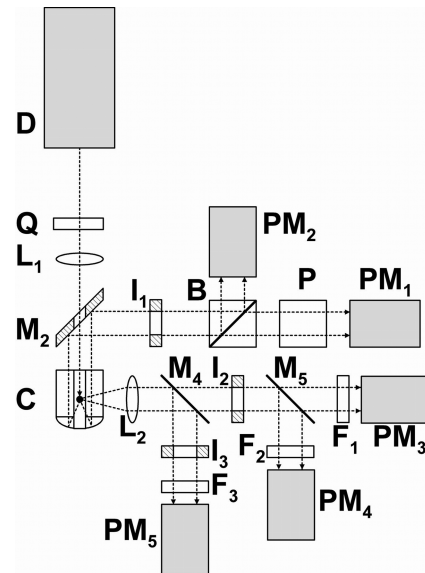


Fig. 1. Optical scheme of the system. The elements are described in Table 1. The three bending mirrors M_1 (inserted between D and Q) and bending mirror M_3 (inserted between M_2 and I_1) are not influential and have not been indicated.

1). In general the optical system of CLASS relating to the light-scattering part tallies with the polarizing scanning flow cytometer [12].

The linearly polarized beam, after having been bent by three mirrors to make the system compact, gets across a quarter-wave plate, going out circularly polarized. Later, after having been focused by a lens and having gotten across a mirror with a hole, the beam coaxially coincides on a flow of particle in liquid suspension that gets across the capillary (254 μm diameter) of a cuvette. In the interaction region (less than 5 mm length), the beam has a small cross section (approximately 30 μm diameter FWHM), and thus the radiant energy flow is high.

The light scattered by the particle is reflected toward the mirror with a hole by the spherical mirror that forms the bottom of the cuvette. The radiation reflected by the mirror with the hole, after having been bent by a mirror to make the system compact, is split into two parts by a nonpolarizing beam splitter. The transmitted part is detected by photomultiplier PM_1 , and after having gotten across a polarizer, reflected one is detected as it is by the photomultiplier PM_2 . The beam splitter, polarizer, and photomultipliers are mounted on an aluminum block, allowing only the light coming from the mirror with the hole to pass. A variable diaphragm performs the spatial filtering of the input beam.

It should be noted that, for each position of the particle along the capillary, only the light coming from a well-defined scattering polar angle is detected, because the radiation collimated by the spherical mirror is observed. Consequently, by retrieving the position from the acquisition time of the signal, thanks to the measurement of the particle velocity and its transit time in a known point, it is possible to determine

Table 1. Optical Elements of the System^a

Element	Description	Characteristics	Producer/Model
D	Diode laser	λ of 405 nm; power of 50 mW; polarization ratio of 100:1	μ LS/Lepton IV
M ₁	Broadband dielectric mirror	\varnothing of 25.4 mm; AOI of 45°; $R > 97\%$ (400–750 nm)	Micos
Q	Zero-order quarter-wave plate	λ of 405 nm; \varnothing of 12.7 mm; AR coating at 405 nm	Micos
L ₁	Plano-convex lens	f of 60 mm; $R < 3\%$ (350–650 nm)	Thorlabs/LA1134 A
M ₂	Broadband dielectric mirror with hole	\varnothing of 25.4 mm; hole \varnothing of 1 mm; $R > 97\%$ (400–750 nm)	Micos
C	Cuvette with spherical mirror	\varnothing of 5 mm; h of 5 mm	ICKC
M ₃	Broadband dielectric mirror	\varnothing of 25.4 mm; AOI of 0°–45°; $R > 98\%$ (400–800 nm)	Thorlabs/BB1-E02
I ₁	Variable iris diaphragm	\varnothing of 2 mm	Thorlabs/D12S
B	Nonpolarizing beam splitter cube	Side 10 mm; T and $R > 40\%$ (400–600 nm)	Thorlabs/BS010
P	Glan Thompson polarizer	CA \varnothing of 10 mm; extinction ratio 100,000:1	Thorlabs/GTH10M
PM ₁	Photomultiplier module	λ of 300–650 nm (peak of 420 nm); sensitivity of 4.3×10^4 A/W. Connected to the amplifier Femto HCA-10M-100K-C	Hamamatsu/H6780
PM ₂	Photomultiplier module	λ of 185–650 nm (peak of 420 nm); sensitivity of 4.3×10^4 A/W. Connected to the amplifier Analog Modules 352-1-B-1M	Hamamatsu/H6780-03
L ₂	Microscope objective	Magnification of 50 \times ; NA of 0.55	Zeiss/LD EC Epiplan-Neofluar
M ₄	Dichroic mirror	\varnothing of 25.4 mm; AOI of 45°; $R > 90\%$ (405 nm); $T > 70\%$ (>435 nm)	Laser Components/630DRLP
I ₂	Variable iris diaphragm	\varnothing of 4 mm	Thorlabs/D12S
M ₅	Dichroic mirror	\varnothing of 25.4 mm; AOI of 45°; $R > 90\%$ (460–620 nm); $T > 70\%$ (>660 nm)	Laser Components/435DRLP
F ₁	Interference filter	\varnothing of 25.4 mm; T of 74% (680 nm); BW of 11 nm	Laser Components/680DF10
PM ₃	Photomultiplier module	λ of 300–900 nm (peak of 630 nm); sensitivity of 3.9×10^4 A/W. Connected to the amplifier Femto HCA-1M-1M-C	Hamamatsu/H6780-20
F ₂	Interference filter	\varnothing of 25.4 mm; T : 64% (530 nm); BW of 6 nm	Omega Optical/530BP5
PM ₄	Photomultiplier module	λ of 185–850 nm (peak of 400 nm); sensitivity of 3.0×10^4 A/W. Connected to the amplifier Femto HCA-1M-1M-C	Hamamatsu/H6780-04
I ₃	Variable iris diaphragm	\varnothing of 1 mm	Thorlabs/D12S
F ₃	Interference filter	\varnothing of 25.4 mm; T of 51% (402 nm); BW of 5 nm	Omega Optical/403BP5
PM ₅	Photomultiplier module	λ of 185–750 nm (peak of 420 nm); sensitivity of 5.2×10^5 A/W. Connected to the amplifier Analog Modules 352-1-B-1M	Hamamatsu/H7710-11

^a λ , wavelength; \varnothing , diameter; AOI, angle of incidence; R , reflectance; AR, antireflection; f , focal length; h , height; NA, numerical aperture; T , transmittance; CA, clear aperture; and BW, bandwidth.

the scattering intensity as a function of the polar angle, the light-scattering profile (LSP) in a wide interval (typically from 5° to 100°). The transit time of the particle in a known point is measured, as we will see, by observing the side scattering. The particle velocity is a previously calibrated function of the pressures in the hydrodynamic circuit.

The system observes the side radiation by a microscope objective. The light is split into three spectral zones by two dichroic mirrors. The reflection of the first dichroic mirror sends the side scattering to photomultiplier PM₅ that measures the transit time of the particle at a known point and provides the trigger to the experiment. The photomultiplier is mounted on an aluminum block allowing only the light coming from the particle to pass. A variable diaphragm and an interference filter perform the spatial and spectral filtering, respectively, of the input beam. The second dichroic mirror

- transmits the red radiation to photomultiplier PM₃ that measures the fluorescence of the

particle approximately 680 nm after spectral filtering with an interference filter, and

- reflects the green radiation toward photomultiplier PM₄ that measures the fluorescence of the particle approximately 530 nm after spectral filtering with an interference filter.

The photomultipliers and the interference filters are mounted on an aluminum block allowing only the light coming from the particle to pass. A variable diaphragm performs spatial filtering of the input beam.

The signals detected by the photomultipliers are amplified by the transimpedance amplifiers indicated in Table 1, digitized by the analog-to-digital converter ADLINK DAQ-2010 (4 channels, 14 bits, 2 MS/s), and eventually stored and analyzed in an industrial personal computer. Once the sample (typically some thousands of particles) is inserted, the system analyzes it in a few minutes, providing fluorescence and the two LSPs used in the evaluation of effective size, effective refractive index, and depolarization of each particle.

A. Mueller Matrix Formalism

The light-scattering signals of CLASS can be described using the Mueller formalism [16]. We can write LSPs I_1 and I_2 at the output of photomultipliers PM_1 and PM_2 (see Fig. 1), respectively, as follows [12]:

$$I_1(\theta) = k \int_0^{2\pi} [S_{11} - S_{14} + (S_{21} - S_{24}) \cos(2\varphi) - (S_{31} - S_{34}) \sin(2\varphi)] d\varphi, \quad (1)$$

$$I_2(\theta) = k \int_0^{2\pi} (S_{11} - S_{14}) d\varphi, \quad (2)$$

where $S_{ij}(\theta, \varphi)$ are the elements of the Mueller light-scattering matrix of an arbitrary particle, θ and φ are the polar and azimuth angles, respectively, measured with respect to the direction of the incident beam (see Fig. 1).

For a spherical particle, Eqs. (1) and (2) become

$$I_1(\theta) = k \int_0^{2\pi} S_{11} d\varphi = 2\pi k S_{11}(\theta), \quad (3)$$

$$I_2(\theta) = k \int_0^{2\pi} S_{11} d\varphi = 2\pi k S_{11}(\theta). \quad (4)$$

If the particles were spherical, signals I_1 and I_2 would be the same (unless a constant factor k was linked to the different efficiencies of the respective detection channels, which can be made equal to one, adjusting the gain of the photomultipliers). Therefore, if a particle is spherical, depolarization

$$\delta I = \frac{I_2 - I_1}{I_2} \quad (5)$$

is zero. In contrast, if a particle is not spherical, the depolarization is

$$\delta I(\theta) = - \frac{\int_0^{2\pi} [(S_{21} - S_{24}) \cos(2\varphi) - (S_{31} - S_{34}) \sin(2\varphi)] d\varphi}{\int_0^{2\pi} (S_{11} - S_{14}) d\varphi}. \quad (6)$$

Consequently the depolarization measurement will allow us to discriminate spherical particles, and this feature is particularly useful for classifying phytoplankton cells.

B. Effective Refractive Index Determination

For homogeneous spheres the refractive index can be determined from the evaluation of the side scattering intensity by a least-squares fit method [5].

Chlamydomonas reinhardtii cells cannot be considered homogeneous spheres, therefore the previously

mentioned method cannot be applied. However, it is possible to estimate their effective refractive index by an alternative empirical method, as illustrated below.

The following integral parameter has been evaluated for each *C. reinhardtii* cell:

$$J = \int_{10^\circ}^{70^\circ} I_2(\theta) \cdot \sin\left(\pi \cdot \frac{\theta - 10^\circ}{60^\circ}\right) d\theta. \quad (7)$$

This parameter has been discovered to have a functional relation with the phase-shift parameter, defined as $\rho = 2\alpha(n/n_0 - 1)$, where $\alpha = \pi d n_0 / \lambda$ is the size parameter, n is the refractive index of the particle, n_0 is the refractive index of the medium, d is the equivalent diameter of the particle, and λ is the wavelength of the incident radiation.

Simulations show (see Fig. 2) the dependency of the phase-shift parameter ρ of a sphere on integral J for size parameter $\alpha = 30, 50, 70, 90, 110$, and 130 (corresponding to $d = 2.9, 4.8, 6.8, 8.7, 10.6$, and $12.5 \mu\text{m}$). For such α values and for $n_0 = 1.33$ (refractive index of water), the range of ρ from 0 to 50 corresponds to a range of n from 1.36 to 1.64.

Regardless of the α value, good single-valued dependency of ρ on J exists only for refractive indices lower than 1.46 (in Fig. 2, the ρ trend for n up to 1.46 is shown by dots). The following equation is selected for the empirical relation between ρ and J :

$$\rho = A J^\beta [1 + k_1(1 + k_2 P_f) J^{2/\beta}], \quad (8)$$

where P_f is the location of the maximum peak in the spectral decomposition of the LSP [17], and A, β, k_1 , and k_2 are fitting coefficients. This choice has been based on some theoretical considerations. In fact, the first term, $A J^\beta$, defines the dependence of ρ on J at small values of ρ and size parameter α , according to the Rayleigh–Gans approximation [18]. The second term, k_1 and $J^{2/\beta}$, can be read as a correction to the main one, taking into account an increment

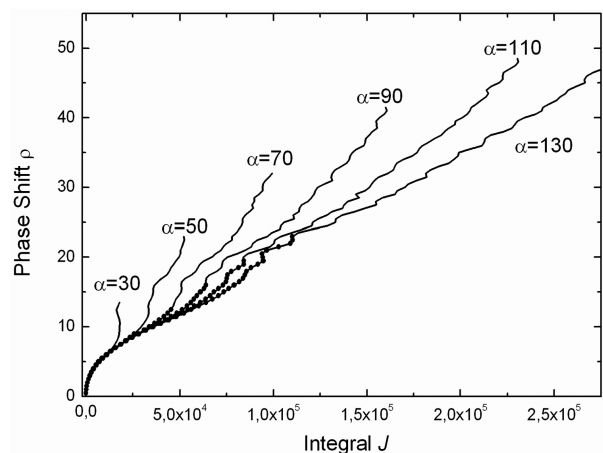


Fig. 2. Dependency of phase-shift parameter ρ on parameter J for different values of size parameter α .

Table 2. Fitting Coefficients of Eq. (8) that Correspond to the Minimum Value of χ^2

Coefficient	Value	Error
A	0.111	0.003
β	0.430	0.003
k_1	2.8×10^{-23}	0.8×10^{-23}
k_2	-1.366	0.007

of the power for the main term with the increase of the J value. The third term, k_2 , P_f , and $J^{2/\beta}$, is a correction considering the dependence of integral J on the size parameter at large values of α .

To obtain the values of the coefficients contained in Eq. (8), a nonlinear fitting procedure is applied. A χ^2 test is used to minimize the residual standard error between the initial ρ values used for the simulations and those calculated by means of Eq. (8), since J and P_f are simulation results. The values of the coefficients are shown in Table 2.

Finally, using the equation found, ρ can be determined from LSP parameters J and P_f with a mean relative error $\varepsilon = 1.7\%$ (when the refractive index of a particle is varied from 1.36 to 1.46 and α is varied from 16 to 125). This method gives a maximum systematic relative error of 5.6% in determination of ρ of a spherical particle from light scattering.

The fitting coefficients for Eq. (8), used for effective refractive index retrieval, are derived from a calibration on homogeneous spheres. For this reason, the calculation of the refractive index of real aspheric, not homogeneous, cells will not be considered accurate in absolute. However, as it will be shown, this method gives a valuable tool to distinguish different kinds of particles, and this is important for cell sorting, which is one of the main goals of this study.

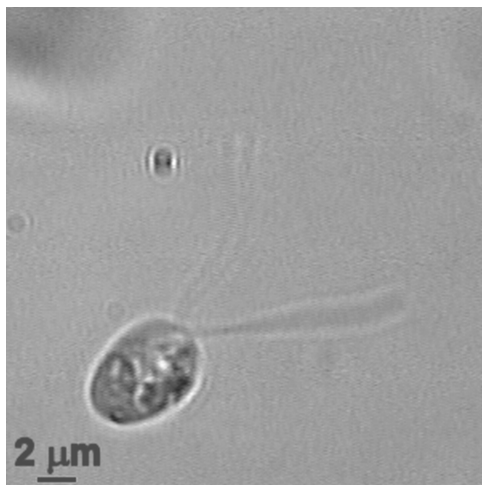


Fig. 3. Images of Chlamydomonas at the optical microscope in Fig. 4 LSPs of Chlamydomonas.

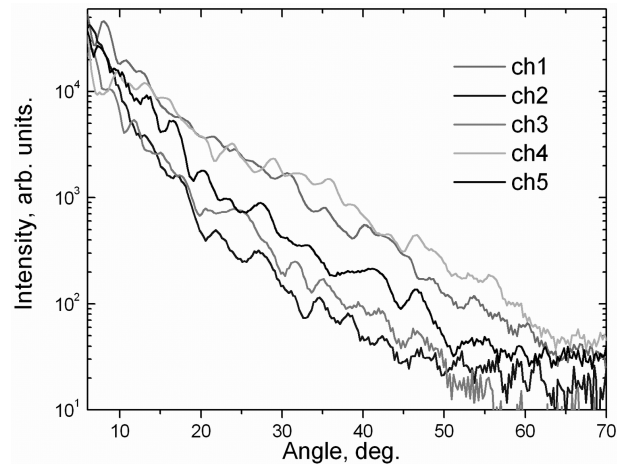


Fig. 4. Images of Chlamydomonas at the optical microscope just before measurement with CLASS.

3. Results and Discussions

We analyzed a sample of *C. reinhardtii*, a eukaryote single-cell green alga, approximately $10 \mu\text{m}$ long, that moves using two flagella, approximately $10 \mu\text{m}$ long (see Fig. 3). This cell offers an ideal test for the system having a spheroid shape and containing chlorophyll a that imply, respectively, nonzero depolarization and fluorescence approximately 680 nm . The mix of polystyrene microspheres Molecular Probes F-13838 (component B, $2 \mu\text{m}$, nonfluorescent) and Molecular Probes A-14836 ($6 \mu\text{m}$, fluorescent at $670\text{--}720$) is used for testing of the possibility of CLASS to measure different types of particle. Some examples of measured LSPs I_2 for *C. reinhardtii* (we will simply call it Chlamydomonas) cells are presented in Fig. 4. The measured LSPs I_2 are used here for determination of effective size and effective refractive index of Chlamydomonas.

Examples of depolarization measured from 5° to 60° for Chlamydomonas and 2 and $6 \mu\text{m}$ polystyrene

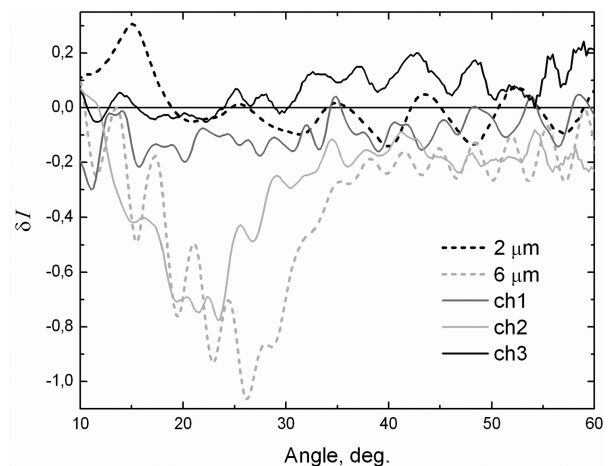


Fig. 5. Depolarization δI for Chlamydomonas and 2 and $6 \mu\text{m}$ polystyrene microspheres.

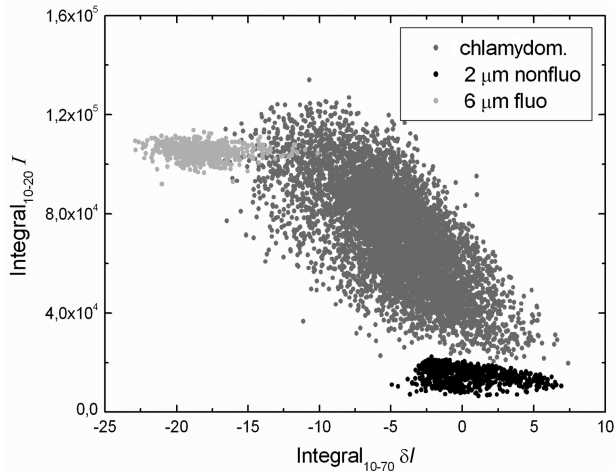


Fig. 6. Two-dimensional scatterplot (LSP integral J in the range of 10° – 20° versus integral of depolarization δI in the range 10° – 70°) obtained analyzing a sample of *Chlamydomonas* mixed with fluorescent polystyrene spheres, having 6 and $2\ \mu\text{m}$ diameters.

microspheres are presented in Fig. 5. To discriminate different particles, the identification of the angle range in which the differences in depolarization signals are the largest is important. In fact, in combination with the accurate choice of LSP parameters, depolarization can be a good tool for cell classification. This is confirmed by the two-dimensional scatterplot of LSP integral J in the range of 10° to 20° versus the integral of depolarization δI in the range from 10° to 70° shown in Fig. 6.

Some results obtained on a sample of *Chlamydomonas* cells mixed with fluorescent and nonfluorescent polystyrene spheres, having 6 and $2\ \mu\text{m}$ diameters, are shown in Table 3 and Fig. 7.

Determination of the effective sizes for microspheres and *Chlamydomonas* are similar and described in [17,19]. The refractive index of *Chlamydomonas* is determined with the method illustrated in Section 2. Unfortunately that method cannot be used to determine the refractive index of microspheres, because polystyrene has a refractive index larger than 1.46. Consequently the refractive index of microspheres has been obtained by a nonlinear least-squares fitting procedure based on the Levenberg–Marquardt algorithm.

First we observe that the system correctly measures the size and the refractive index of the polystyrene particles. In fact, the expected values of 2.0 and $5.7\ \mu\text{m}$ for the sizes and 1.604 for the refractive index at a wavelength of 405 nm (according to Molecular Probes documentation and Ref. [20], respectively) are close to the measured ones: $2.09\ \mu\text{m}$ (standard deviation [SD] $0.01\ \mu\text{m}$) and $5.61\ \mu\text{m}$ (SD $0.01\ \mu\text{m}$) for the diameters and 1.593 (SD 0.006), 1.598 (SD 0.002) for the refractive indices.

The three-dimensional projection scatterplot in Fig. 8 shows how useful depolarization and fluorescence measurements are for the accurate classification of microscopic particles; without them, it would have been impossible to fully distinguish cells and spheres.

To give an example of the usefulness of the fluorescence observation in two different spectral bands, it has been studied in a sample prepared by mixing green fluorescent and nonfluorescent polystyrene spheres, having a $2\ \mu\text{m}$ diameter (indicated as $2\ \mu\text{m}$ F and $2\ \mu\text{m}$ NF, respectively), with red fluorescent and nonfluorescent polystyrene spheres having a $6\ \mu\text{m}$ diameter (indicated as $6\ \mu\text{m}$ F and $6\ \mu\text{m}$ NF, respectively). The three-dimensional scatterplot shown in Fig. 9 demonstrates that CLASS resolves the four types of particle in well-distinct clouds of points.

4. Conclusions

A new laser flow cytometer (CLASS) has been developed. Its more relevant feature is the introduction of a polarized source and the detection of unpolarized and linearly polarized scattered light for identification of phytoplankton. Thanks to that innovation, simultaneous measurements of effective size, refractive index, depolarization, and fluorescence of microscopic particles have been carried out. To our knowledge they represent the first example of those results by LFC.

The tests carried out on polystyrene spheres show that some thousands of particles can be analyzed in a few minutes and indicate that the accuracy of CLASS in the retrieval of effective size and refractive index can exceed 1%.

CLASS has been applied to the experimental characterization of phytoplankton cells. That research confirms the role of fluorescence measurements, and more importantly, demonstrates the role of depolarization measurements in the classifi-

Table 3. Measurements of the Effective Size, the Effective Refractive Index, the Depolarization, and the Fluorescence Obtained Analyzing a Sample of *C. Reinhardtii* Mixed with Fluorescent and Nonfluorescent Polystyrene Spheres, Having 6 and $2\ \mu\text{m}$ Diameters^a

Particle	Number	Size [μm]		Refractive Index		Depolarization [a.u.]		Fluorescence [a.u.]	
		M	SD	M	SD	M	SD	M	SD
<i>Chlamydomonas</i>	6567	8.86	1.65	1.4291	0.0211	-5.17	4.12	41	13
$6\ \mu\text{m}$ F	779	5.61	0.01	1.5983	0.0026	-18.20	1.96	73	5
$2\ \mu\text{m}$ NF	734	2.09	0.01	1.5933	0.0057	0.00	2.23	0.3	0.1

^aM is mean, and SD is standard deviation.

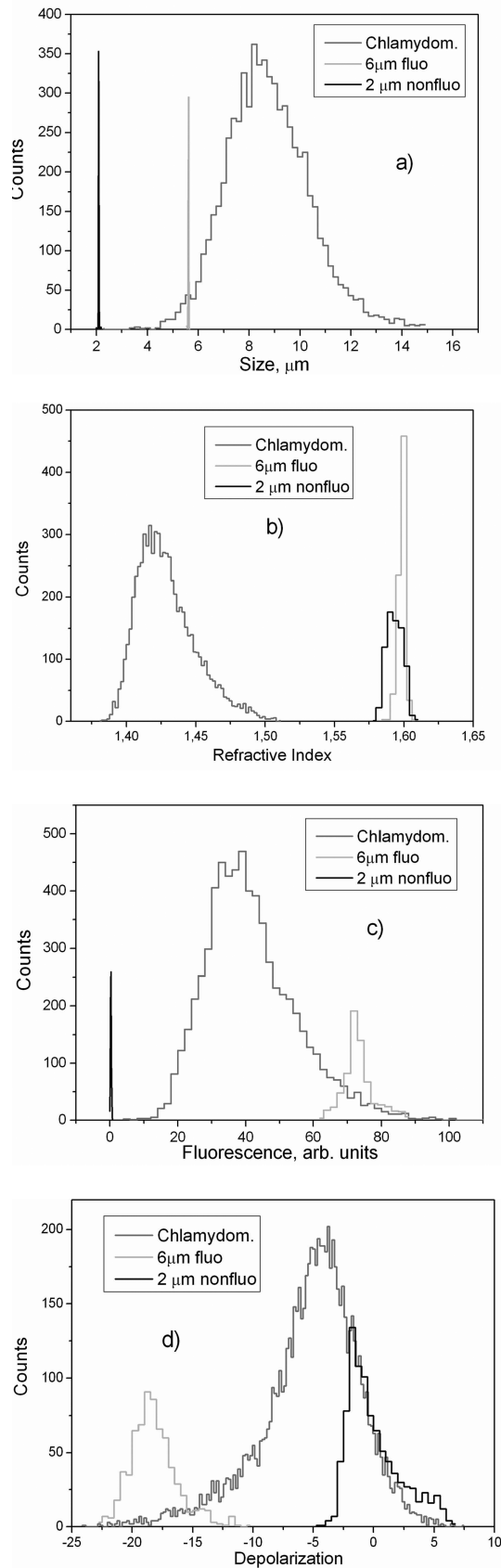


Fig. 7. Histograms of (a) size, (b) refractive index, (c) fluorescence, and (d) depolarization obtained analyzing a sample of Chlamydomonas mixed with fluorescent and nonfluorescent polystyrene spheres, having 6 and 2 μm diameters.

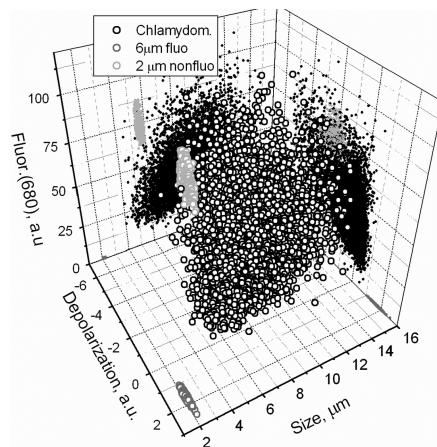


Fig. 8. Three-dimensional scatterplot (effective size, depolarization, and fluorescence) obtained analyzing a sample of Chlamydomonas mixed with fluorescent and nonfluorescent polystyrene spheres, having 6 and 2 μm diameters.

cation of particles otherwise indistinguishable by size and refractive index determination.

The authors are deeply grateful to R. Fantoni for the constant encouragement. Special thanks to P. Aristipini for technical drawings, R. Giovagnoli for mechanical parts, F. Barnaba for system tests, and P. Albertano for Chlamydomonas samples. The help of A. Lai and M. Sighicelli (biological laboratory) is gratefully acknowledged. This work has been supported by the Italian Ministry of University and Research within the framework of the project Microsystems for Hostile Environments and by the Siberian Branch of the Russian Academy of Sciences through grants 2006-45 and 2006-3. K. A. Semyanov acknowledges support of INTAS Postdoctoral Young Scientist Fellowship Ref. No. 05-109-5148.

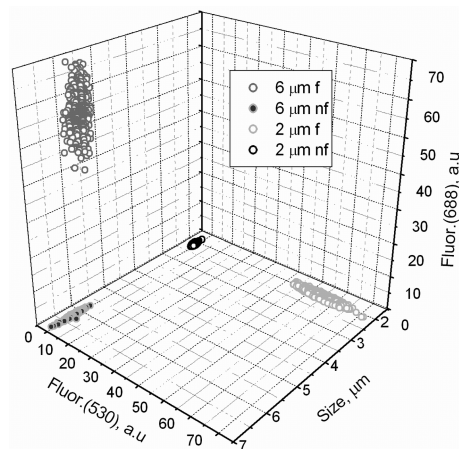


Fig. 9. Three-dimensional scatterplot (size, fluorescence at 530 nm, and fluorescence at 680 nm) obtained analyzing a sample prepared mixing green fluorescent and nonfluorescent polystyrene spheres, having a 2 μm diameter, with red fluorescent and nonfluorescent polystyrene spheres, having a 6 μm diameter.

References

1. L. Tsang, J. A. Kong, and K.-H. Ding, *Scattering of Electromagnetic Waves: Theories and Applications* (Wiley, 2001).
2. T. Provder and J. Texter, eds., *Particle Sizing and Characterization* (American Chemical Society, 2004).
3. H. M. Shapiro, *Practical Flow Cytometry* (Wiley, 2003).
4. D. E. Burger, J. H. Jett, and P. F. Mullaney, "Extraction of morphological features from biological models and cells by Fourier analysis of static light scatter measurements," *Cytometry* **2**, 327–336 (1982).
5. G. C. Salzman, P. F. Mullaney, and B. J. Price, "Light-scattering approaches to cell characterization," in *Flow Cytometry and Sorting*, M. R. Melamed, T. Lindmo, and M. Mendelsohn, eds. (Wiley, 1979).
6. G. B. J. Dubelaar and R. R. Jonker, "Flow cytometry as a tool for the study of phytoplankton," *Sci. Mar.* **64**, 135–156 (2000).
7. T. J. O'Leary, "Flow cytometry in diagnostic cytology," *Diagn. Cytopathol.* **18**, 41–46 (1998).
8. L. Fiorani and A. Palucci, "Local and remote laser sensing of bio-optical parameters in natural waters," *J. Comput. Technol.* **11**, 39–45 (2006).
9. L. Fiorani, *Une Première Mesure Lidar Combinée d'Ozone et de Vent, À Partir d'Une Instrumentation et d'Une Méthodologie Coup par Coup* (Swiss Federal Institute of Technology, 1996).
10. A. V. Chernyshev, V. I. Prots, A. A. Doroshkin, and V. P. Maltsev, "Measurement of scattering properties of individual particles with a scanning flow cytometer," *Appl. Opt.* **34**, 6301–6305 (1995).
11. V. P. Maltsev, "Scanning flow cytometry for individual particle analysis," *Rev. Sci. Instrum.* **71**, 243–255 (2000).
12. V. P. Maltsev and K. A. Semyanov, *Characterisation of Bio-Particles from Light Scattering*, Inverse and Ill-Posed Problems Series (VSP, 2004).
13. P. Aristipini, L. Fiorani, I. Menicucci, and A. Palucci, "Spettrofluorimetro laser portatile per l'analisi *in situ* dei liquidi non opachi," Italian patent RM2005A000269 (30 May 2005).
14. V. P. Maltsev and A. V. Chernyshev, "Method and device for determination of parameters of individual microparticles," U.S. patent 5,650,847 (22 July 1997).
15. F. Barnaba, L. Fiorani, A. Palucci, and P. Tarasov, "First characterization of marine particles by laser scanning flow cytometry," *J. Quant. Spectrosc. Radiat. Transfer* **102**, 11–17 (2006).
16. R. Guenther, *Modern Optics* (Wiley, 1990).
17. K. A. Semyanov, P. A. Tarasov, A. E. Zharinov, A. V. Chernyshev, A. G. Hoekstra, and V. P. Maltsev, "Single-particle sizing from light scattering by spectral decomposition," *Appl. Opt.* **43**, 5110–5115 (2004).
18. C. F. Bohren and D. R. Huffman, *Absorption and Scattering of Light by Small Particles* (Wiley-Interscience, 1983).
19. K. A. Semyanov, A. E. Zharinov, P. A. Tarasov, M. A. Yurkin, I. G. Skribunov, D. R. van Bockstaele, A. G. Hoekstra, and V. P. Maltsev, "Optics of leucocytes," in *Optics of Biological Particles*, A. G. Hoekstra, V. P. Maltsev, and G. Videen, eds. (Springer, 2006), pp. 253–264, ISBN 978-1-4020-5501-0.
20. X. Y. Ma, J. Q. Lu, R. S. Brock, K. M. Jacobs, P. Yang, and X. H. Hu, "Determination of complex refractive index of polystyrene microspheres from 370 to 1610 nm," *Phys. Med. Biol.* **48**, 4165–4172 (2003).